Localization of Point Targets from Cortical Waves Using ARMA Models

Wenxue Wang*, Bijoy K. Ghosh**
Department of Electrical and Systems Engineering, Washington University
St. Louis, MO 63130
ww1@zach.wustl.edu
ghosh@netra.wustl.edu

Philip S. Ulinski
Committee on Computational Neuroscience,
The University of Chicago, Chicago, IL 60637
pulinski@uchicago.edu

***Abstract*— Visual stimuli elicit waves of activity that propagate across the visual cortex of turtles. It is believed that these activity waves encode features of the visual stimuli, viz. position and velocity of targets. An important problem is to estimate the target location from the activity waves of the visual cortex. In this paper, we have used a large scale model of the turtle visual cortex to simulate the response of the cortex to stationary and moving visual stimuli. Subsequently, we have estimated the position and velocity of the target from the neural activities of the cortex by constructing an Autoregressive and Moving Average (ARMA) Model. The input to the model is the neuronal response suitably smoothed by a low pass filter. The output of the ARMA model is precisely the prediction of the cortical inputs. This paper illustrates the role of ARMA models in deciphering the location and velocity of visual targets from the associated cortical waves.**

I. INTRODUCTION

The visual cortex of a turtle responds to signals from the natural visual scenes. It is well known that the cortex, when stimulated by an input pattern of visual activity, produces waves of cellular activities. These activities have been experimentally observed, assuming a stationary and a moving flash as an input, by Prechtl, Cohen, Mitra, Pesaran and Kleinfeld 1997 and by Senseman 1996. A large scale model of the cortex, the NGU model (see Nenadic, Ghosh and Ulinski 2000, 2002), has also been constructed with the software package, called GENESIS (Bower and Beeman, 1998), that has the ability to simulate cortical waves with the same qualitative features as the cortical waves seen in experimental preparations. Nenadic, Ghosh and Ulinski (2000, 2002, 2003) and Du and Ghosh (2003) studied the dynamics as well as estimation and detection problems of the activity of waves by stimulating the NGU cortex model with inputs of flash patterns. It is believed that the activity waves of a turtle visual cortex encode features of the visual stimuli, viz. position, and velocity of targets. Wang, Ghosh and Ulinski (2003, 2004) modified the NGU model by adding another type of inhibitory neurons, the subpial cells, to produce the new WUNG model. The purpose of this paper is to estimate the cortical inputs from the associated neural responses by constructing an Autoregressive and Moving Average model and then detect the location of targets or velocity of target motion with estimates of the cortical inputs. For the purpose of this study, a set of cortical responses were simulated to stationary visual inputs at different locations and moving visual inputs with different starting positions and different velocities. The cortical activities of pyramidal cells were smoothed with a low pass filter. The smoothed activities of the pyramidal cells are considered as inputs to an ARMA model to detect the location or velocity of targets. Fig 1 shows the schematic diagram of the detection process from the cortical activity.

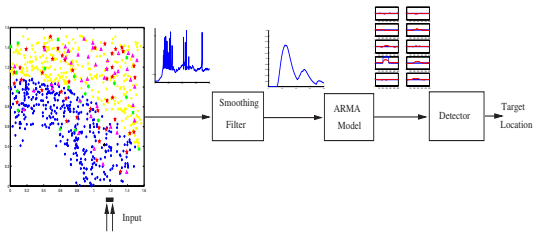

Fig. 1. System Diagram

II. SIMULATION OF THE VISUAL CORTEX MODEL

The model of the visual cortex contains an array of 201 lateral geniculate neurons (LGN) along the lateral edge of the cortex. To simplify the inverse problem, a point target in the visual space, is simulated by electrical activation of a cluster of 20 LGN neurons. Stationary stimuli are simulated by presenting a 150ms square current pulse to the geniculate neurons in a cluster. Moving stimuli are simulated by presenting 150ms square current pulses to the geniculate neurons in different clusters with certain time delay/velocity. In this study, three cases were considered: a single stationary target, double stationary targets, and moving targets. In the case of a single stationary target, visual stimuli were chosen at 19 different positions and 19 associated cortical responses were simulated. The visual stimuli locate from left to right with clusters of LGN neurons indexed by $10(k-1)+1,...,10(k+1)$ corresponding to normalized positions $0.05, 0.10, ..., 0.95$, where $k =$

*Research was partially supported from NSF grant ECS-9976174
**Research was partially supported from NSF grants ECS-9976174, and ECS-0323693

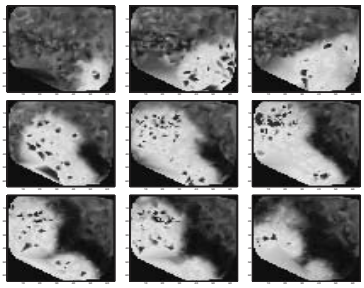

Fig. 2. 9 snapshots selected from a representative cortex movie at 60, 150, 180, 300, 330, 380, 500, 550, and 660 and 350 ms respectively

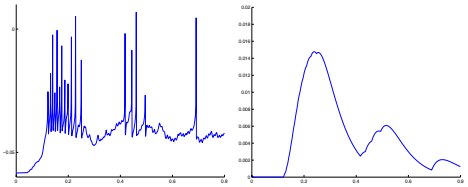

Fig. 3. the cortical response and the smoothed activity of a representative pyramidal cell

$1,2,...,19$, along the array of LGN neurons. In the case of double stationary targets, the two targets are located at any pair of clusters, which do not overlap, among the 10 clusters of LGN neurons indexed by $20(k-1)+1,...,20k$, where $k=1,2,...,10$. A total of 45 choices of double stationary stimuli have generated 45 cortical responses. In the case of moving stimuli, the moving patterns of a target were simulated by stimulating the LGN neurons of 6 continuous clusters with square current pulses with a certain amount of time delay. In this study, the choices of time delay are 20ms, 40ms and 60ms. The target moves from left to right or from right to left. So a total of 30 moving stimuli were chosen that generated 30 cortical responses. The cortical response of the visual cortex can be viewed as movies by spatial interpolation of the voltage values between neurons at each time. Fig 2 shows 9 movie snapshots from a representative movie. The cortical responses were smoothed with a low pass filter. Fig 3 shows the cortical response and the smoothed activity of a representative pyramidal cell.

III. Estimation of the Location and Velocity of Targets

So far, we have stated that visual stimuli induce waves of activity in the model cortex. We represent this wave as a spatiotemporal signal $M(x,t)$. The activities of the cells (pyramidal) of the cortex encode features of the visual input such as the location and velocity of the targets. An important inverse problem is to 'Decode the features of the visual input from the activity waves of the model cortex.' In this paper, the detection of the location and velocity of targets from the responses of the turtle visual cortex consists of two steps. In step 1, we estimate the visual stimuli from the responses of the visual cortex and in step 2, we detect

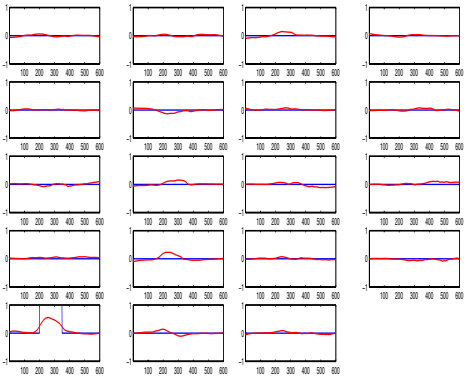

Fig. 4. The estimate of the visual stimulus fed to LGN neurons 81 to 100(a single stationary target). Red lines are the actual signals, and blue ones are the estimated signals

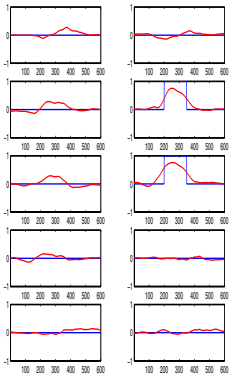

Fig. 5. The estimate of the visual stimulus fed to LGN neurons 61 to 80 and 101 to 120 (double stationary target). Red lines are the actual signals, and blue ones are the estimated signals

the location and velocity of targets from the estimated visual stimuli. The details are described as follows.

A. Estimation of the visual stimuli from the responses of the visual cortex

In the visual cortex model, the activities $r_m(t)$ of 679 pyramidal cells, where m indexes the pyramidal cells, encode the features of the visual inputs. In other words, the activities of pyramidal cells directly encode the square currents which were considered as inputs to the cortex model. So the first step in detection of the location and velocity of targets is to estimate the visual stimuli. The responses of pyramidal cells were filtered with a second order low pass filter and the smoothed activities were used to estimate the visual stimuli. Because the dimension of the activities, 679, is too high to estimate the visual stimuli, the activities were clustered locally. The cortical space was subdivided evenly into $8\times 8=64$ small square patches and the average activity of the cells in every patch was obtained. Excluding those patches without any pyramidal cells or with average activity close to zero, 42 average activities from other patches were used in the estimation of the visual stimuli. An ARMA model (see Goodwin and Sin, 1984),

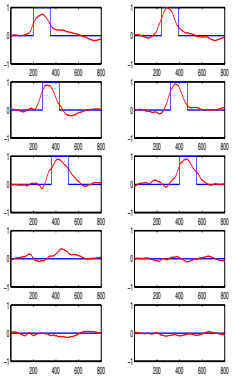

Fig. 6. The estimate of the moving visual stimulus from the cluster of LGN neurons 1 through 20 to the cluster of LGN neurons 101 through 120 (moving target from left to right with 40ms time delay). Red lines are the actual signals, and blue ones are the estimated signals

with the average neural activities as input and the associated visual stimulus to the model of the visual cortex as output with 200ms time delay, was chosen for the estimation of the visual stimuli. The 200ms time delay makes the ARMA model causal. In this study, the ARMA model used is 2^{nd} order and is described as

$$\begin{aligned} y(t) &= -A_1 y(t-1) - A_2 y(t-2) \\ &\quad + B_1 u(t-1) + B_2 u(t-2) \end{aligned}$$

where $y(t)$ and $u(t)$ are output and input respectively. In this paper, we have:

$$\begin{aligned} \hat{V}_k(t) &= -A_1 \hat{V}_k(t-1) - A_2 \hat{V}_k(t-2) \\ &\quad + B_1 R_k(t-1) + B_2 R_k(t-2) \end{aligned}$$

where k indexes the visual stimuli, $\hat{V}_k(t)$ is the estimate of visual stimuli and $R_k(t)$ is the average activity vector of 42 dimensions. The parameter matrices A_1, A_2, B_1, and B_2 were trained respectively for 3 cases using the Matlab Identification Toolbox. There are 19 output signals from the ARMA model for the case of a single stationary target, and 10 output signals for the the case of double stationary targets and the case of moving targets. Fig 4, Fig 5 and Fig 6 show the the examples of the estimates of the visual stimuli to the model of the visual cortex for 3 cases respectively.

B. Detection of the location and motion of targets from the estimated visual stimuli

Above, the estimation of the visual stimuli from the average activities of the pyramidal cells was discussed. In this section, the estimated visual stimuli were used to detect the location or motion of targets. For the case of a single stationary target, the maximal sum of signal values of a 100ms time window were calculated by sliding the window of 100ms within the interval between 200ms and 350ms for each of 19 output signals. The location of the target was detected by comparing the 19 maximal sums and taking the maximum of the 19 sums. Fig 7 shows the detected

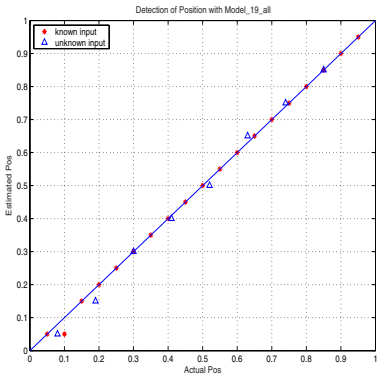

Fig. 7. the detected locations versus the actual locations of the targets for the case of a single stationary target

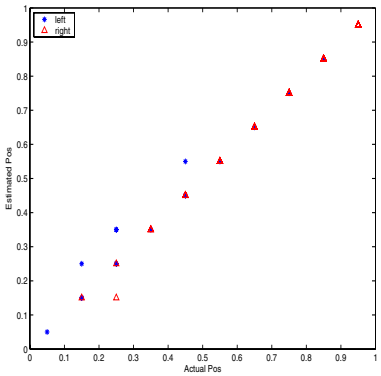

Fig. 8. the detected locations versus the actual locations of the left and right targets for the case of double stationary targets

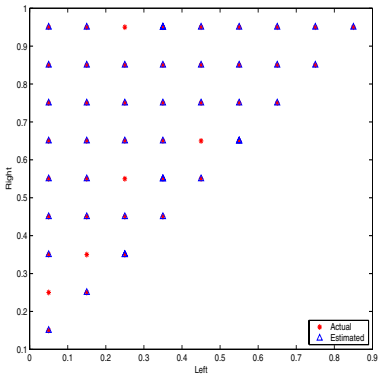

Fig. 9. the detected and actual locations of the right target versus the locations of the left targets for the case of double stationary targets

Actual Location	Estimated Location	Error
(0.05 0.15)	(0.05 0.15)	(0 0)
(0.05 0.25)	(0.05 0.15)	(0 -0.10)
(0.05 0.35)	(0.05 0.35)	(0 0)
(0.05 0.45)	(0.05 0.45)	(0 0)
(0.05 0.55)	(0.05 0.55)	(0 0)
(0.05 0.65)	(0.05 0.65)	(0 0)
(0.05 0.75)	(0.05 0.75)	(0 0)
(0.05 0.85)	(0.05 0.85)	(0 0)
(0.05 0.95)	(0.05 0.95)	(0 0)
(0.15 0.25)	(0.15 0.25)	(0 0)
(0.15 0.35)	(0.25 0.35)	(0.10 0)
(0.15 0.45)	(0.15 0.45)	(0 0)
(0.15 0.55)	(0.15 0.55)	(0 0)
(0.15 0.65)	(0.15 0.65)	(0 0)
(0.15 0.75)	(0.15 0.75)	(0 0)
(0.15 0.85)	(0.15 0.85)	(0 0)
(0.15 0.95)	(0.15 0.95)	(0 0)
(0.25 0.35)	(0.25 0.35)	(0 0)
(0.25 0.45)	(0.25 0.45)	(0 0)
(0.25 0.55)	(0.35 0.55)	(0.10 0)
(0.25 0.65)	(0.25 0.65)	(0 0)
(0.25 0.75)	(0.25 0.75)	(0 0)
(0.25 0.85)	(0.25 0.85)	(0 0)
(0.25 0.95)	(0.35 0.95)	(0.10 0)
(0.35 0.45)	(0.35 0.45)	(0 0)
(0.35 0.55)	(0.35 0.55)	(0 0)
(0.35 0.65)	(0.35 0.65)	(0 0)
(0.35 0.75)	(0.35 0.75)	(0 0)
(0.35 0.85)	(0.35 0.85)	(0 0)
(0.35 0.95)	(0.35 0.95)	(0 0)
(0.45 0.55)	(0.45 0.55)	(0 0)
(0.45 0.65)	(0.55 0.65)	(0.10 0)
(0.45 0.75)	(0.45 0.75)	(0 0)
(0.45 0.85)	(0.45 0.85)	(0 0)
(0.45 0.95)	(0.45 0.95)	(0 0)
(0.55 0.65)	(0.55 0.65)	(0 0)
(0.55 0.75)	(0.55 0.75)	(0 0)
(0.55 0.85)	(0.55 0.85)	(0 0)
(0.55 0.95)	(0.55 0.95)	(0 0)
(0.65 0.75)	(0.65 0.75)	(0 0)
(0.65 0.85)	(0.65 0.85)	(0 0)
(0.65 0.95)	(0.65 0.95)	(0 0)
(0.75 0.85)	(0.75 0.85)	(0 0)
(0.75 0.95)	(0.75 0.95)	(0 0)
(0.85 0.95)	(0.85 0.95)	(0 0)

TABLE I

ACTUAL AND ESTIMATED LOCATIONS OF THE DOUBLE TARGETS

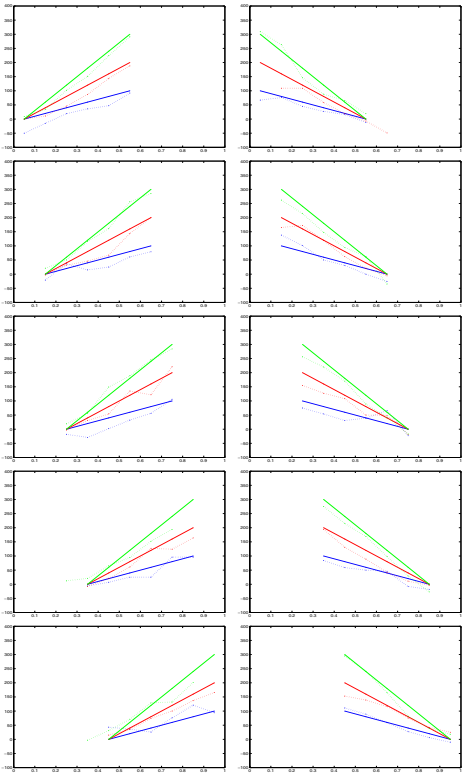

Fig. 10. the detected and actual arriving times of the moving targets versus the locations for the case of moving targets. Left column is for the motions with direction from left to right, and in this column, from top to bottom are the motions with starting position $0.05, 0.15, 0.25, 0.35,$ and 0.45. Right column is for the motions with direction from right to left, and in this column, from top to bottom are the motions with starting position $0.55, 0.65, 0.75, 0.85,$ and 0.95. the colors blue,red, and green refer the time delays of 20ms,40ms, and 60ms respectively. Solid lines refer the actual and dotted lines refer the estimated

locations versus the actual locations of the targets for the case of a single stationary target. The known inputs are the visual stimuli which were used to train the ARMA model. The unknown inputs are the visual stimuli which were used to test the ARMA model. For the case of double stationary targets, the locations of the two targets were detected by taking the first two maximal values from the 10 sums, which were calculated by sliding the window of 100ms within the interval between 200ms and 350ms for each of 10 output signals. Fig 8 shows the detected locations versus the actual locations of the targets for the case of double stationary targets. Fig 9 shows the detected and actual locations of the right targets versus the locations of the left targets for the case of double stationary target. Table I gives the actual and estimated locations of the double targets. In the every pair of data, the first one is the position of the left target, and the second one is the position of the right target. The errors were obtained by subtracting the actual values from the estimated ones. For the case of moving targets, the maximal sum of signal values of a 100ms time window were calculated by sliding the window of 100ms from 200ms for each of the 10 output signals. The first 6 maximal values were taken by comparing the 10 sums. The corresponding times when the target arrived at the location were estimated by taking the middle times of the sliding windows where the maximal sums were obtained and then subtracting 275ms from the middle times. Fig 10 shows the detected and actual arriving times of the moving target versus the locations for the case of moving targets. Table II gives the actual starting positions and time delays of the moving stimuli, and the estimated starting positions and average time delays of the associated moving stimuli. In the every pair of data, the first one is the starting position of the target, and the second one is the time delay of the motion. The errors were obtained by subtracting the actual values from the estimated ones.

Actual	Estimated	Error	Relative Error
(0.05 20.00)	(0.05 28.40)	(0 8.40)	0.4200
(0.05 40.00)	(0.05 37.60)	(0 -2.40)	0.0600
(0.05 60.00)	(0.05 56.40)	(0 -3.60)	0.0600
(0.15 20.00)	(0.15 20.00)	(0 0)	0
(0.15 40.00)	(0.15 40.60)	(0 0.60)	0.0150
(0.15 60.00)	(0.15 52.80)	(0 -7.20)	0.1200
(0.25 20.00)	(0.25 24.80)	(0 4.80)	0.2400
(0.25 40.00)	(0.25 44.80)	(0 4.80)	0.1200
(0.25 60.00)	(0.25 53.00)	(0 -7.00)	0.1167
(0.35 20.00)	(0.35 20.40)	(0 0.40)	0.0200
(0.35 40.00)	(0.35 34.40)	(0 -5.60)	0.1400
(0.35 60.00)	(0.25 36.40)	(-0.1 -23.60)	0.3933
(0.45 20.00)	(0.45 10.20)	(0 -9.80)	0.4900
(0.45 40.00)	(0.45 30.20)	(0 -9.80)	0.2450
(0.45 60.00)	(0.35 40.80)	(-0.1 -19.20)	0.3200
(0.55 20.00)	(0.55 15.80)	(0 -4.20)	0.2100
(0.55 40.00)	(0.65 31.60)	(0.1 -8.40)	0.2100
(0.55 60.00)	(0.55 58.00)	(0 -2.00)	0.0333
(0.65 20.00)	(0.65 32.80)	(0 12.80)	0.6400
(0.65 40.00)	(0.65 34.20)	(0 -5.80)	0.1450
(0.65 60.00)	(0.65 59.40)	(0 -0.60)	0.0100
(0.75 20.00)	(0.75 19.60)	(0 -0.40)	0.0200
(0.75 40.00)	(0.75 34.60)	(0 -5.40)	0.1350
(0.75 60.00)	(0.75 54.60)	(0 -5.40)	0.0900
(0.85 20.00)	(0.85 20.40)	(0 0.40)	0.0200
(0.85 40.00)	(0.85 39.60)	(0 -0.40)	0.0100
(0.85 60.00)	(0.85 60.40)	(0 0.40)	0.0067
(0.95 20.00)	(0.95 24.20)	(0 4.20)	0.2100
(0.95 40.00)	(0.95 25.60)	(0 -14.40)	0.3600
(0.95 60.00)	(0.95 55.40)	(0 -4.60)	0.0767

TABLE II

ACTUAL AND ESTIMATED MOTION OF THE TARGETS

IV. RESULTS

In the above section, the estimation of the locations of the stationary targets, and the motions of moving targets was discussed in 3 cases. In the case of a single stationary target, the locations of the known target were detected very well. 18 of the 19 locations were detected accurately and the one at 0.10 was wrongly detected with error 0.05. The locations of the unknown visual stimuli were also detected well with detecting error less than 0.05. This point can be seen in Fig 7. In the case of double stationary targets, 40 of the 45 pairs of targets were detected precisely. The rest 5 pairs of targets were wrongly detected with the detecting error 0.10. The point can be seen in Fig 8, Fig 9, and Table I. In the case of moving targets, among 30 moving stimuli chosen for the study, only three stimuli got wrong detection of the starting positions of the target motion. This can be clearly seen in Table II. Moving directions of the most targets were estimated correctly, and few of the targets got wrong estimation of moving directions which are associated with the non-monotonic curves in Fig 10. The time delay of the most moving stimuli were estimated with relative errors less than 0.25. Only 6 of the 30 visual stimuli got the estimation of the time delay with relative errors larger than 0.25. Table II shows the point. Overall, the features of visual stimuli can be detected very well from the activity waves of the visual cortex with an ARMA model. This study also shows that the visual cortex plays an important role in encoding information on visual inputs.

REFERENCES

[1] J. M. Bower and D. Beeman, *The Book of Genesis*, (TELOS, Santa Clara, 1998).

[2] X. Du and B. K. Ghosh, "Decoding the position of a visual stimulus from the cortical waves of turtles ", Proceedings of the American Control Conference, (2003).

[3] G. C. Goodwin and K. S. Sin, *Adaptive Filtering Prediction and Control*, (PRENTICE-HALL, 1984).

[4] P. Z. Mazurskaya, "Organization of receptive fields in the forebrain of *Emys orbicularis*", *Neurosci. Behav. Physiol.*, vol. 7, pp. 311–318, (1974).

[5] Z. Nenadic, B. K. Ghosh and P. Ulinski, "Spatiotemporal dynamics in a model of turtle visual cortex", *Neurocomputing,*, 32–33, pp. 479–486,(2000).

[6] Z. Nenadic, B. K. Ghosh and P. Ulinski, "Modeling and estimation problems in the turtle visual cortex", *IEEE Trans. on Biomedical Engineering*, vol. 49, no. 8, pp. 753–762, (2002).

[7] Z. Nenadic, B. K. Ghosh and P. Ulinski, "Propagating waves in visual cortex: A large scale model of turtle visual cortex", *J. Computational Neuroscience,* Vol. 14, pp. 161-184, (2003).

[8] B. A. Olshausen and D. J. Field, "Sparse coding with an overcomplete basis set: A strategy employed by V1?", *Vision Res.,* Vol. 37, No. 23, pp. 3311–3325, (1997).

[9] J. C. Prechtl, "Visual motion induces synchronous oscillations in turtle visual cortex", *Proc. Natl. Acad. Sci.* USA 91: 12467–12471, 1994.

[10] J. C. Prechtl, T. H. Bullock and D. Kleinfeld, "Direct evidence for local oscillatory current sources and intracortical phase gradients in turtle visual cortex", *Proc. Natl. Acad. Sci.* 97: 877–882, 2000.

[11] J. C. Prechtl, L. B. Cohen, P. P. Mitra, B. Pesaran and D. Kleinfeld, "Visual stimuli induce waves of electrical activity in turtle cortex", *Proc. Natl. Acad. Sci.* 94: 7621–7626, 1997.

[12] K. A. Robbins and D. M. Senseman, "Visualizing differences in movies of cortical activity", *IEEE Trans. Visualization Compt. Graphics*, vol. 4, pp. 217–224, 1998.

[13] D. M. Senseman, "Correspondence between visually evoked voltage sensitive dye signals and activity recorded in cortical pyramidal cells with intracellular microelectrodes", *Vis. Neurosci.*, vol. 13, pp. 963–977, 1996.

[14] D. M. Senseman and K. A. Robbins, "Modal behavior of cortical neural networks during visual processing", *J. Neuroscience*, vol. 19, RC3, pp. 1–7, (1999).

[15] P. S. Ulinski, W. Wang and B. K. Ghosh, "Generation and Control of Propagating Waves in the Visual Cortex", *In 42nd IEEE Conference on Decision and Control*, (2003).

[16] W. Wang, B. K. Ghosh and P. S. Ulinski, "Integrative Physiology of Subpial Cells", Submitted to *Journal of Computational Neuroscience,* (2004).